Excitation of true polar wander by subduction

Giorgio Spada*†, Yanick Ricard* & Roberto Sabadini†

* Département de Géologie, de l'Ecole Normale Supérieure, 75231 Paris, France
† Istituto di Geofisica, Dipartimento di Fisica, Università di Bologna, 40127 Bologna, Italy

TRUE polar wander—the global motion of the mantle relative to the Earth's rotation axis—is known from the analysis of palaeomagnetic data, hotspot tracks and plate motions to have occurred at velocities of up to 0.5° Myr^{-1} since the Late Cretaceous period[1–4]. We address here the longstanding question of how fast episodes of true polar wander (TPW) can be excited[5], by analysing the impact of the distribution and activity of subduction zones on polar motion. Using nonlinear Liouville equations, which allow us to treat large excursions of the polar axis, we show that unrealistically fast TPW is excited by subduction episodes unless the lower mantle has a viscosity at least 10 times that of the upper mantle. This need for a viscosity increase with depth in the mantle reinforces the conclusions of previous studies on post-glacial rebound and geoid anomalies, theoretical creep laws and some preliminary results on TPW induced by density anomalies embedded in the mantle[6–10]. The lower viscosity in the upper mantle means that upper-mantle density anomalies are most effective in exciting TPW. Changes in the pattern of subduction through time may be responsible for both episodes of fast TPW and times of quiescence in polar motion.

The 1969 paper of Goldreich and Toomre[11] renewed the interest of the geophysical community[12] in the role of polar wandering in Earth's dynamics. Their example of a colony of beetles crawling on the surface of a quasi-rigid Earth suggests that large excursions of the axis of rotation with respect to the entire mantle could be produced by small redistributions of matter. A large amount of TPW can be caused by the cumulative effects of the random walk of tiny density features, mimicking drifting lithospheric plates[11].

Goldreich and Toomre made two main approximations, neglecting isostatic compensation and the Earth's equatorial bulge. These two approximations, valid for a quasi-rigid planet, are abandoned here as we use a viscoelastic stratified model. When mantle rheology is considered, isostasy cancels the inertial perturbations associated with surface tectonic features so that drifting plates cannot excite polar wander. On the contrary, geoid anomalies suggest that mantle density heterogeneities embedded sufficiently far away from chemical interfaces, such as the Earth's surface, the core–mantle boundary (CMB) or the 660-km discontinuity, induce the main perturbation of the inertia tensor[13–15].

To understand the effect of mantle mass redistribution in exciting TPW, we solve the nonlinear Liouville equations that govern the Earth's rotation in the case of inertia perturbations due to time-dependent subduction processes. The inertia tensor $J_{ij}(t)$ of a rotating body can be organized as follows[16]

$$J_{ij}(t) = I\delta_{ij} + \frac{k^{T}(t)a^{5}}{3G}[\omega_i(t)\omega_j(t) - \tfrac{1}{3}\omega^2(t)\delta_{ij}] + [\delta(t) + k^{L}(t)]C_{ij}(t) \quad (1)$$

where ω_i denotes the components of the angular velocity vector in a geographical frame, G the gravitational constant, a the Earth's radius and I the inertia of the non-rotating planet. A perturbation $C_{ij}(t)$ acts instantaneously through a Dirac delta function $\delta(t)$ and has a delayed response expressed by the convolution with the loading Love number $k^{L}(t)$ (ref. 17). The viscous readjustment of the equatorial bulge is described by the term containing the tidal Love number $k^{T}(t)$. For a viscoelastic planet, the two Love numbers k^{L} and k^{T}, characterized by a set of modes and their own relaxation times, are obtained by means of classic analytical techniques[18] and account for the response of the Earth to loading and tidal potentials. For a model consisting of an elastic lithosphere, an upper and lower mantle described by a viscoelastic Maxwell rheology, and an inviscid core[19], the time dependence of the Love numbers introduces into the Liouville equations widely separated timescales ranging from the fast Chandler wobble oscillation to the relaxation over several million years of internal chemical boundaries[14,15,20]. These various characteristic times prohibit any numerical treatment of the Liouville equations unless some approximation is made. As the subduction zones only evolve with a timescale of a few million years, we perform an asymptotic expansion of the two Love numbers for large time. Such an expansion filters the fast modes and allows us to solve the Liouville equation by a Runge–Kutta scheme.

We model the subduction processes by the sinking of point sources of mass 2×10^{19} kg in the mantle. This corresponds to a slab pull of 5×10^{13} N m^{-1} along a trench[21] whose total length is 4×10^{3} km. The inaccuracy in the inertia tensor due to the use of point masses instead of extended slabs is negligible. We

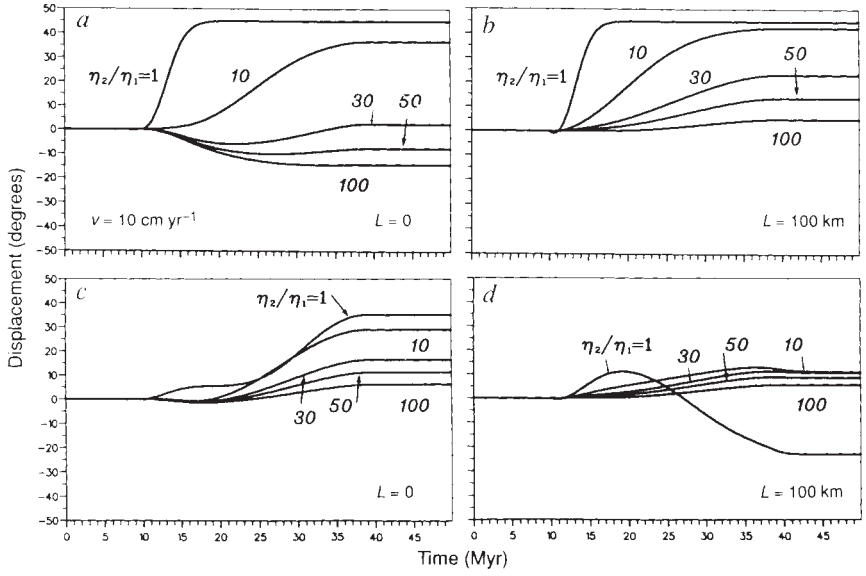

FIG. 1 Displacement of the axis of rotation for a mass anomaly sinking at a constant rate of 10 cm yr^{-1} down to the CMB, for varying viscosity ratio η_2/η_1. The initial latitude of the source, activated at $t=10$ Myr, is 45° *a*, *b*, Phase-change transition at 660 km depth; *c*, *d*, Chemical boundary with a density jump[19] $\Delta\rho/\rho=9\%$. The lithosphere is absent in *a* and *c*, whereas its thickness is fixed at 100 km in *b* and *d*.

impose $C_{ii}(t) = 0$ to conserve the average inertia of the Earth[22] and its mass.

Figure 1 portrays the angular displacement $m = \arccos(\omega_1/\Omega)$ (in degrees, where Ω denotes the diurnal angular velocity) of the axis of rotation induced by a single subducting slab activated at 10 Myr at a latitude of 45° and sinking at a velocity of 10 cm yr^{-1} down to the CMB. The upper-mantle viscosity η_1 is kept to 10^{21} Pa s, while the lower-mantle viscosity η_2 is varied from η_1 to $100\eta_1$. Panels *a* and *b* correspond to boundary conditions at the upper-lower mantle interface appropriate for a fully adiabatic phase-change transition. A non-adiabatic chemical transition at 660 km is modelled in panels *c* and *d*. In such a stratified mantle the slab does not penetrate the lower mantle. We assume, however, for the sake of simplicity, that thermal coupling through the 660-km interface induces a cold, sinking blob with the mass of the slab. The lithosphere is absent in Fig. 1 *a* and *c* with $L = 0$, whereas its thickness is fixed at 100 km in Fig. 1 *b* and *d*.

We choose the convention that positive TPW values denote a drift toward the mass anomaly. There is a dominance of such motions that indicates that the inertia associated with topography generated by compensation on top of the slab generally overcomes the inertia perturbation due to the slab itself. Surface compensation is inhibited to some extent by the hardening of the lower mantle, and for $\eta_2/\eta_1 = 50$, $L = 0$ (ref. 8), the rotation pole is forced in the opposite direction (Fig. 1*a*). The perturbations in the moment of inertia are associated with the geoid components of degree 2 (ref. 10) and the rotation pole wanders toward a geoid low and away from a geoid high. In an isoviscous adiabatic mantle, the pole position is highly unstable, as shown by the rapid 45° displacement in Fig. 1*a*. Viscosity increase with depth or chemical stratification reduces the displacement amplitude and increases the time span needed to attain the equilibrium. Linearized Liouville equations, considered previously[10], are correct only for the small excursions of the axis of rotation occurring in the early stages of subduction (Fig. 8 of ref. 10) and cannot be used to model realistic subduction episodes which can in principle cause large amounts of TPW, as shown in this figure.

We can now generalize the results of Goldreich and Toomre[11] by computing the pole displacement generated by a random distribution of density anomalies that model episodic subduction processes in a viscously stratified Earth. Such a model of mass redistribution is simplified, but we think that it captures the main physical ingredients of TPW induced by real subductions.

We consider subduction episodes activated every $\Delta t = 2$ Myr (Fig. 2*a*–*d*) and every $\Delta t = 10$ Myr (Fig. 2*e*, *f*). Their geographical coordinates are chosen by means of a random number generator. The process of density anomaly generation is interrupted at 500 Myr. The slab velocities in the upper mantle are 10 cm yr^{-1} except for the dotted lines of Fig. 2*e* and *f* where they have been reduced to 5 cm yr^{-1}. The value of 10 cm yr^{-1}, an upper bound for the present-day subduction pattern, is appropriate for the Late Cretaceous, when plate velocities and spreading rates were generally higher[23,24]. In all these computations, the mantle is adiabatically stratified and the slab velocities are diminished in the lower mantle in accordance with the viscosity increase.

Figure 2*a* and *b* shows, for a mantle with uniform viscosity, the absolute velocity V and the three components of the angular velocity vector ω_i/Ω in the geographical coordinate frame with the North Pole coincident with the rotation pole at $t = 0$. Their values are extremely sensitive to the distribution of the internal density anomalies. The TPW velocity can be as high as 15° Myr^{-1} during the periods of largest rotational instabilities. This is much larger than the value inferred from palaeomagnetic studies, 0.5° Myr^{-1}, indicated by a horizontal arrow.

For $\eta_2/\eta_1 = 10$ the mantle flow is inhibited and the average pole velocity is lowered to ~0.5° Myr^{-1} (Fig. 2*c*, *d*). The spikes are smoother than in Fig. 2*a*, about 1° Myr^{-1}, because of the enhanced rotational stability. The transient of about 50 Myr (Fig. 2*c*, *d*) is a consequence of the initial lack of any isotropy in the geographical distribution of subductions; this effect is also visible in Fig. 2*a* and *b*, on a shorter timescale because of the lower viscosity. Another deviation from the results of the isoviscous mantle is the decreased variability in the velocity V and in the ω_i/Ω components, after most of the subducting slabs have crossed the 660-km viscosity discontinuity at 500 Myr.

In Fig. 2*e* and *f* the interval Δt between subduction episodes is increased to 10 Myr, the largest time interval that ensures that at least one subduction is always active in the upper mantle, even with a sinking velocity of 5 cm yr^{-1}. The number of subduction episodes is kept constant so that the process of subduction generation covers the whole time window shown in the figure.

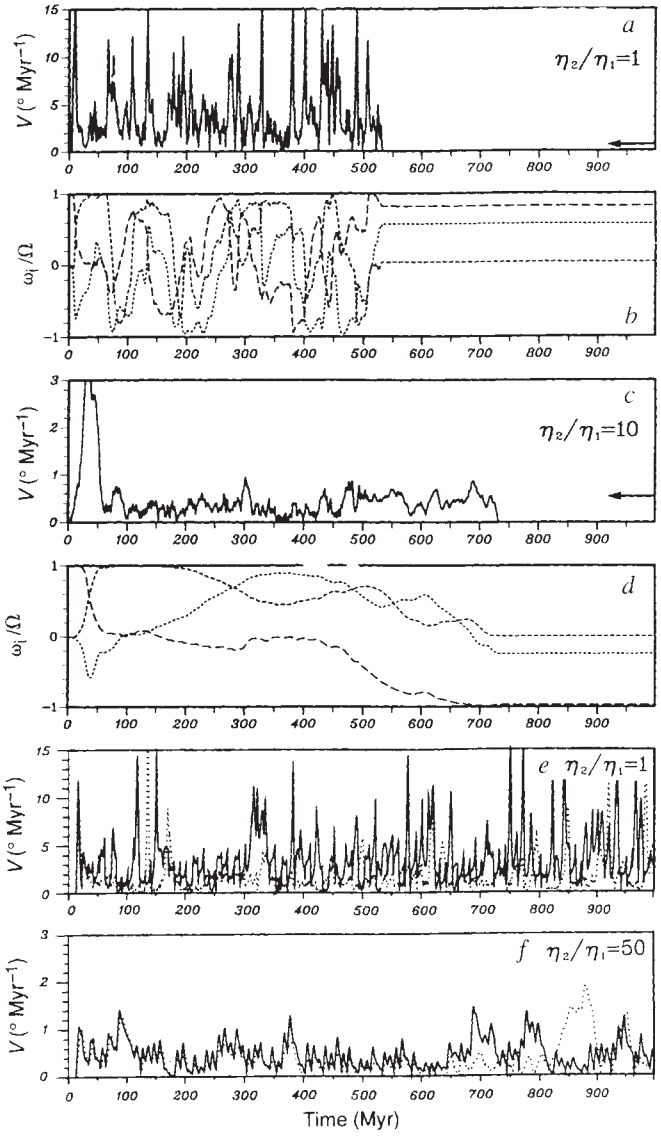

FIG. 2 *a*–*d*, Absolute value of polar wander velocity V (° Myr^{-1}) and *b*, *d*, normalized components of the angular velocity vector ω_i/Ω, for different lower-mantle viscosities and phase-change transition; the dotted curves in *b* and *d* denote the equatorial components of the angular velocity vector while the dashed ones stand for the polar component. The velocity of the blobs in the lower mantle is reduced in accordance with the viscosity increase. In *a* and *d*, density anomalies are activated randomly every 2 Myr, whereas in *e* and *f*, Δt is increased to 10 Myr. $\eta_2/\eta_1 = 1$ in *a*, *b* and *e*, $\eta_2/\eta_1 = 10$ in *c* and *d*, and $\eta_2/\eta_1 = 50$ in *f*. Dotted curves in *e*, *f* stand for sinking velocity of 5 cm yr^{-1}. The horizontal arrows denote the TPW velocity inferred from observations[1–3].

Comparison with Fig. 2*a* indicates that the results are essentially insensitive to the activation time Δt of subduction episodes, suggesting that TPW is controlled by the timescale associated with the readjustment of the equatorial bulge. We verified that with $\Delta t = 50$ Myr the subducting slabs do not interact and the case of the single episode of Fig. 1 is retrieved. A decrease in the slab velocity to 5 cm yr^{-1} (dotted) reduces the TPW for the uniform mantle as shown in Fig. 2*e*. This velocity, however, is still much larger than that observed. A large viscosity increase (Fig. 2*f*) suppresses this dependence of TPW on the sinking velocity of the slabs.

The 660-km transition is treated as a chemical boundary in Fig. 3. For $\eta_2/\eta_1 = 1$ or 10 the results are similar to the phase-change models of Fig. 2, the peak values for the velocity are generally smaller. The chemical boundary reduces the mantle flow, decreasing the variability of the moment of inertia. This effect is more pronounced when the lower-mantle viscosity is increased (Fig. 2 *e*, *f*). After all the density anomalies have entered the highly viscous lower mantle, the Earth becomes stable and the random characteristics of the pole path tend to vanish (Fig. 2*f*). The decoupling of the mantle flow, enhanced by the chemical density jump, acts as a stabilizing factor when the density anomalies are still active in the upper mantle.

These results show that changes in the geographical distribution of subduction zones could induce considerable polar wander. The viscosity profile and the density contrasts at 660 km depth control the TPW. The observations suggest that the lower-mantle viscosity should be at least 10^{22} Pa s. The hardening below 660 km shields the upper mantle and damps the flow forced by lower-mantle density anomalies, suppressing their effects on TPW. Chemical stratification enhances this behaviour. Our findings provide the geodynamical basis for the interpretation of the fast TPW during the early Tertiary, synchronous with major tectonic events that led to a marked increase in the length of collisional plate boundaries and changes in the location of subduction zones[3,25]. Standstills in TPW are not necessarily related to a reduction in global tectonic activity, but rather to random anomalous density distributions with vanishing total moment of inertia. □

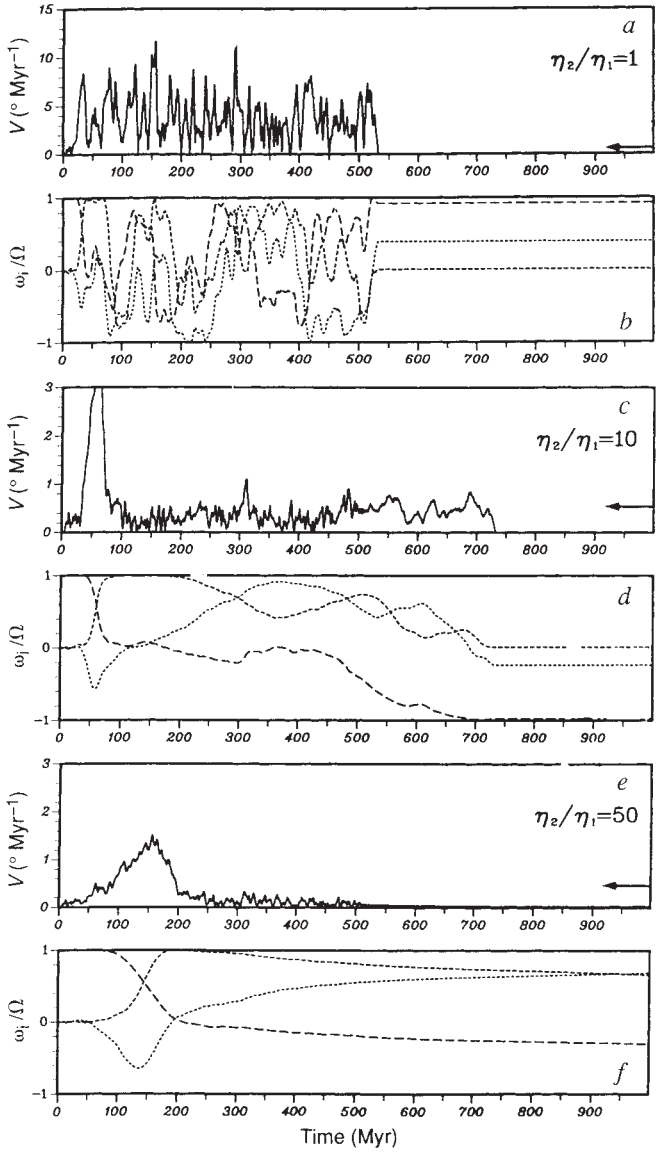

FIG. 3 *a–d*, Same as in Fig. 2 except for non-adiabatic boundary conditions at 660 depth with $\Delta\rho/\rho = 9\%$. In *e* and *f*, the viscosity contrast η_2/η_1 is increased to 50.

Received 17 March; accepted 1 October 1992.

1. Gordon, R. G. & Livermore, R. A. *Geophys. J. R. astr. Soc.* **91,** 1049–1057 (1987).
2. Sager, W. W. & Bleil, U. *Nature* **326**, 488–490 (1987).
3. Courtillot, V. & Besse, J. *Science* **237,** 1140–1147 (1987).
4. Hargraves, R. B. & Duncan, R. A. Nature **245,** 361–363 (1973).
5. Gold, T. *Nature* **175,** 526–529, (1955).
6. Nakada, M. & Lambeck, K. *Geophys. J. int.* **96,** 497–517 (1989).
7. Spada, G., Yuen, D. A., Sabadini, R. & Boschi, E. *Nature* **351,** 53–55 (1991).
8. Ricard, Y., Vigny, C. & Froidevaux, C. *J. geophys. Res.* **94** 13739–13754 (1989).
9. Ranalli, G. in *Glacial Isostasy, Sea-level and Mantle Rheology* (eds Sabadini, R., Lambeck, K. & Boschi, E.) 343–378 (Kluwer, Dordrecht, 1991).
10. Ricard, Y., Sabadini, R. & Spada, G. *J. geophys. Res.* **97,** 14223–14236 (1992).
11. Goldreich, P. & Toomre, A. *J. geophys. Res.* **74,** 2555–2567 (1969).
12. Morgan, W. J. in *The Sea*, Vol. 7 (ed. Emiliani, C.) 443–487 (Wiley, New York, 1981).
13. Sabadini, R. & Yuen, D. A. *Nature* **339,** 373–375 (1989).
14. Richards, M. A. & Hager, B. H. *J. geophys. Res.* **89,** 5987–6002 (1984).
15. Ricard, Y., Fleitout, L. & Froidevaux, C. *Ann. Geophys.* **2,** 267–286 (1984).
16. Sabadini, R. & Peltier, W. R. *Geophys. J. R. astr. Soc.* **66,** 553–578 (1981).
17. Takeuchi, H., Saito, M. & Kobayashi, N. *J. geophys. Res.* **67,** 1141–1154 (1962).
18. Spada, G., Yuen, D. A., Sabadini, R., Morin, P. J. & Gasperini, P. *Math. J.* **1,** 65–69 (1990).
19. Yuen, D. A., Sabadini, R. & Boschi, E. *J. geophys. Res.*, **87,** 10745–10762 (1982).
20. Spada, G., Sabadini, R., Yuen, D. A. & Ricard, Y. *Geophys. J. int.* **109,** 683–700 (1992).
21. Turcotte, D. L. & Shubert, G. *Geodynamics* (Wiley, New York, 1982).
22. Rochester, M. G. & Smylie, D. E. *J. geophys. Res.* **79,** 4948–4951 (1974).
23. Gordon, R. G. & Jurdy, D. M. *J. geophys. Res.* **91,** 12389–12406 (1986).
24. Kominz, M. A. in *Interregional Unconformities and Hydrocarbon Accumulation* (ed. Schlee, J. S.) Am. Assoc. Petr. Geol. Mem. **36,** 109–127 (Tulsa, 1984).
25. Rona, P. A. & Richardson, E. S. *Earth planet. Sci. Lett.* **40,** 1–11 (1978).

ACKNOWLEDGEMENTS. We thank S. Dickman for suggestions. This work was supported by the SCIENCE programme of the EEC.

Mats of giant sulphur bacteria on deep-sea sediments due to fluctuating hydrothermal flow

Jens K. Gundersen*, Bo Barker Jørgensen†, Einer Larsen‡ & Holger W. Jannasch§

* Institute of Biological Sciences, Department of Microbial Ecology, University of Aarhus, 8000 Aarhus C, Denmark
† Max Planck Institute for Marine Microbiology, Fahrenheitstrasse 1, 2800 Bremen 33, Germany
‡ Institute of Biological Sciences, Department of Zoophysiology, University of Aarhus, 8000 Aarhus C, Denmark
§ Department of Biology, Woods Hole Oceanographic Institution, Woods Hole, Massachusetts 02543, USA

FILAMENTOUS sulphide-oxidizing bacteria, *Beggiatoa* spp., commonly grow as submillimetre-thin white films on anoxic marine sediments. Unusually thick mats (>1 cm) of giant *Beggiatoa* filaments, 41–120 μm wide and 2–10 mm long, were observed at 2,000 m water depth in the hydrothermal vent fields of Guaymas Basin, Gulf of California[1–4]. We investigated how such dense communities of the largest known bacteria overcome severe diffusion limitation of their substrate supply, and what advantage